LETTER

doi:10.1038/nature11362

Targeting nuclear RNA for *in vivo* correction of myotonic dystrophy

Thurman M. Wheeler[1,2], Andrew J. Leger[3], Sanjay K. Pandey[4], A. Robert MacLeod[4], Masayuki Nakamori[1,2], Seng H. Cheng[3], Bruce M. Wentworth[3], C. Frank Bennett[4] & Charles A. Thornton[1,2]

Antisense oligonucleotides (ASOs) hold promise for gene-specific knockdown in diseases that involve RNA or protein gain-of-function effects. In the hereditary degenerative disease myotonic dystrophy type 1 (DM1), transcripts from the mutant allele contain an expanded CUG repeat[1–3] and are retained in the nucleus[4,5]. The mutant RNA exerts a toxic gain-of-function effect[6], making it an appropriate target for therapeutic ASOs. However, despite improvements in ASO chemistry and design, systemic use of ASOs is limited because uptake in many tissues, including skeletal and cardiac muscle, is not sufficient to silence target messenger RNAs[7,8]. Here we show that nuclear-retained transcripts containing expanded CUG (CUG^{exp}) repeats are unusually sensitive to antisense silencing. In a transgenic mouse model of DM1, systemic administration of ASOs caused a rapid knockdown of CUG^{exp} RNA in skeletal muscle, correcting the physiological, histopathologic and transcriptomic features of the disease. The effect was sustained for up to 1 year after treatment was discontinued. Systemically administered ASOs were also effective for muscle knockdown of *Malat1*, a long non-coding RNA (lncRNA) that is retained in the nucleus[9]. These results provide a general strategy to correct RNA gain-of-function effects and to modulate the expression of expanded repeats, lncRNAs and other transcripts with prolonged nuclear residence.

Antisense silencing by the RNase H-dependent mechanism entails a three-step process of oligonucleotide hybridization to its cognate RNA, cleavage of the target by RNase H1 and exonuclease degradation of the cleavage fragments. The relative efficiency of this mechanism in the nucleus and cytoplasm is uncertain. Observations that ASOs shuttle from cytoplasm to nucleus[10] and that targeting intronic sequences[11] or nuclear RNA[12] can silence gene expression indicate that antisense is active in the nucleus. However, activity in the cytoplasm is less clear. Although RNase H1 is not restricted to the nucleus[13], recent studies indicate that the non-nuclear fraction is confined to mitochondria[14]. This suggests that ASO•RNase H cleavage is mainly a nuclear process, whose potency could be maximized by targeting transcripts with long nuclear residence.

To test this idea, we used a transgenic mouse model of DM1. HSA^{LR} transgenic mice express CUG^{exp} RNA at high levels in skeletal muscle. Human DM1 is caused by an expanded CTG repeat in the 3′ untranslated region (UTR) of dystrophia myotonica-protein kinase (*DMPK*)[3], whereas in HSA^{LR} mice the expanded repeat is in the 3′ UTR of a human skeletal actin (h*ACTA1*) transgene[6]. In both conditions the CUG^{exp} transcripts are retained in nuclear foci, along with splicing factors in the muscleblind-like (MBNL) protein family. Muscleblind sequestration leads to misregulated alternative splicing and other changes of the muscle transcriptome[15–17]. The RNA toxicity was mitigated in mice by CAG-repeat morpholino oligomers that compete with MBNL proteins for CUG^{exp} binding, without activating RNase H. However, this approach required direct injection into a single muscle, followed by *in vivo* electroporation, a method to load muscle fibres with oligomers[18]. As an alternative, RNase H-active ASOs could produce widespread correction, provided that uptake of circulating ASOs was sufficient to induce target cleavage.

We identified ASOs showing a strong knockdown of h*ACTA1* in tissue culture, good tolerability when systemically administered in wild-type mice, and activity against h*ACTA1*-CUG^{exp} transcripts *in vivo* when electroporated into muscle (Supplementary Figs 1–3). The ASOs had 2′-*O*-methoxyethyl (MOE) modifications at both ends to maximize biostability, and a central gap of 10 unmodified nucleotides to support RNase H activity (MOE gapmers; Supplementary Table 1). We tested three of the ASOs in HSA^{LR} transgenic mice by subcutaneous injection of 25 mg kg^{-1} twice weekly (Fig. 1a). After 4 weeks of administration (8 injections), ASO 445236 reduced the level of CUG^{exp} RNA in hindlimb muscles by more than 80% (Fig. 1b). Another ASO targeting the 3′ UTR, downstream of the repeat tract, also showed strong CUG^{exp} reduction, whereas an ASO targeting the 5′ UTR, or three oligonucleotides against other targets, had no effect (Fig. 1b, c).

RNase H cleavage of mRNA is usually followed by rapid decay of cleavage fragments. However, stable cleavage fragments are observed occasionally[19], and the CUG^{exp} tract forms extensive hairpins[20] and ribonucleoprotein complexes[21] that could inhibit exonuclease activity. The failure of antisense targeting in the 5′ UTR also raised the possibility that cleavage downstream of the repeat tract was required for efficient silencing. We therefore tested an additional ASO, 190401, targeting the h*ACTA1* coding region, and found that it also was highly effective (Fig. 1d). Furthermore, northern blot analysis using a CAG-repeat probe showed no evidence for a stable CUG^{exp} cleavage fragment (Fig. 1e), and *in situ* hybridization showed reduction of nuclear CUG^{exp} foci (Supplementary Fig. 4). These results indicate that expanded CUG repeats are degraded after a cleavage event 5′ or 3′ of the repeat tract.

Reduction of CUG^{exp} RNA would be expected to release sequestered MBNL1 protein and improve its splicing regulatory activity. Consistent with this prediction, alternative splicing of four MBNL1-dependent exons, *Serca1* (also known as *Atp2a1*) exon 22, titin (*Ttn*) exon 362, *Zasp* (also known as *Ldb3*) exon 11, and *Clcn1* chloride ion channel exon 7a, was normalized (Fig. 1f, g and Supplementary Figs 5 and 6)[15]. The *Clcn1* splicing defect causes loss of channel function, repetitive action potentials and delayed muscle relaxation (myotonia)[22], a cardinal feature of the disease. Blind analysis showed that myotonic discharges in hindlimb muscles were eliminated by the active ASOs (Fig. 1h), indicating rescue of *Clcn1* function.

In addition to splicing defects, expression of CUG^{exp} RNA or ablation of *Mbnl1* causes extensive remodelling of the muscle transcriptome[16,17,23]. We used microarrays to examine transcriptomic effects of ASOs. Principle component analysis showed that gene expression in ASO-treated HSA^{LR} mice was shifted towards wild-type mice, indicating an overall trend for transcriptome normalization (Fig. 2a). Among transcripts that were up- or downregulated in HSA^{LR} muscle, more

[1]Department of Neurology, University of Rochester, 601 Elmwood Avenue, Rochester, New York, 14642, USA. [2]Center for Neural Development and Disease, University of Rochester, 601 Elmwood Avenue, Rochester, New York, 14642, USA. [3]Genzyme Corporation, 49 New York Avenue, Framingham, Massachusetts 01701, USA. [4]Isis Pharmaceuticals, 2855 Gazelle Court, Carlsbad, California 92010, USA.

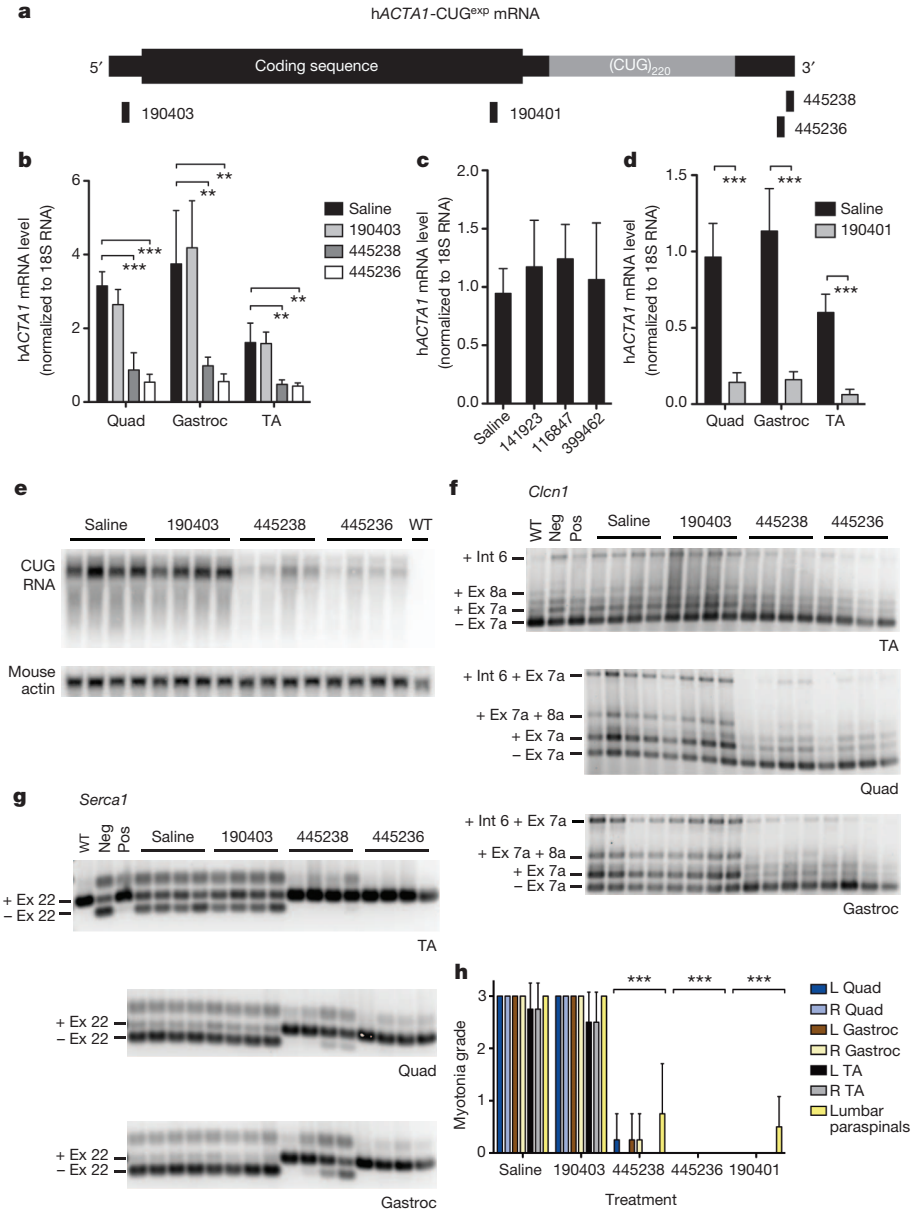

Figure 1 | Systemic administration of 2′-*O*-(2-methoxyethyl) ASOs in the *HSA*^{LR} transgenic mouse model of DM1. **a**, Location of ASO-targeting sequences relative to the h*ACTA1* coding region and the expanded CUG repeat in the 3′ UTR. **b**, Quantitative real-time RT–PCR of h*ACTA1*-CUG^{exp} mRNA in quadriceps (Quad), gastrocnemius (Gastroc) and tibialis anterior (TA) muscle in *HSA*^{LR} mice treated with the indicated ASOs by subcutaneous injection of 25 mg kg^{-1} twice weekly for 4 weeks. Muscle tissue was obtained 1 week after the final dose ($n = 4$ per group). The mean levels of transgene mRNA ± s.d. are shown. $^{**}P < 0.001$, $^{***}P < 0.0001$ (one-way analysis of variance (ANOVA)). **c**, h*ACTA1*-CUG^{exp} transcript levels in quadriceps are not affected by ASOs targeting unrelated transcripts (141923, randomer; 116847, *Pten*; 399462, *Malat1*; $n = 4$ per group; same dose as in **b**). Error bars are mean ± s.d. **d**, Knockdown of h*ACTA1*-CUG^{exp} mRNA in muscle by ASO 190401 ($n = 4$ per group; same dose as in **b**). Error bars are mean ± s.d. $^{***}P \leq 0.0005$ (*t*-test). **e**, Northern analysis of RNA from quadriceps muscle. CUG^{exp} RNA was detected using a $(CAG)_9$ oligonucleotide probe. Mouse actin serves as loading control. **f, g**, RT–PCR analysis of alternative splicing of *Clcn1* (**f**) and *Serca1* (**g**) transcripts. For *Clcn1*, only the –ex7a isoform encodes a functional ion channel. –ex7a, exon 7a exclusion; +ex7a, exon 7a inclusion; –ex22, exon 22 exclusion; +ex22, exon 22 inclusion; neg, negative control mice injected with GAC25 morpholino; pos, positive control mice injected with CAG25 morpholino; WT, FVB/N wild-type mice. **h**, Blind analysis of myotonia using EMG, 1 week after the final dose ($n = 4$ mice per group). Error bars are mean ± s.d. $^{***}P < 0.0001$ for ASO-treated versus saline-treated muscles (two-way ANOVA).

than 85% were normalized or partially corrected by ASOs, without evidence of off-target effects (Fig. 2b, and Supplementary Fig. 7 and Supplementary Table 2). These results confirm that ASOs caused an overall improvement of the muscle transcriptome.

ASO effects were evident within 2 weeks (Supplementary Fig. 8) and were dose-dependent. A threefold dose reduction (8.5 mg kg^{-1} biweekly for 4 weeks) caused partial myotonia and splicing correction, whereas a tenfold dose reduction (2.5 mg kg^{-1}) caused partial myotonia correction in tibialis anterior but not in quadriceps (Supplementary Fig. 9a–c), the latter muscle having higher basal levels of CUG^{exp} expression[18]. Serum chemistries showed no evidence for renal or liver toxicity (Supplementary Fig. 10).

A uniform finding in previous studies of MOE gapmer ASOs was that systemic administration failed to cause significant target reduction in muscle, despite efficient knockdown in liver ($n = 12$ different mRNA targets; Supplementary Table 3), raising the possibility that muscle tissue in our model is unusually susceptible to antisense silencing. We examined the functional integrity of the muscle

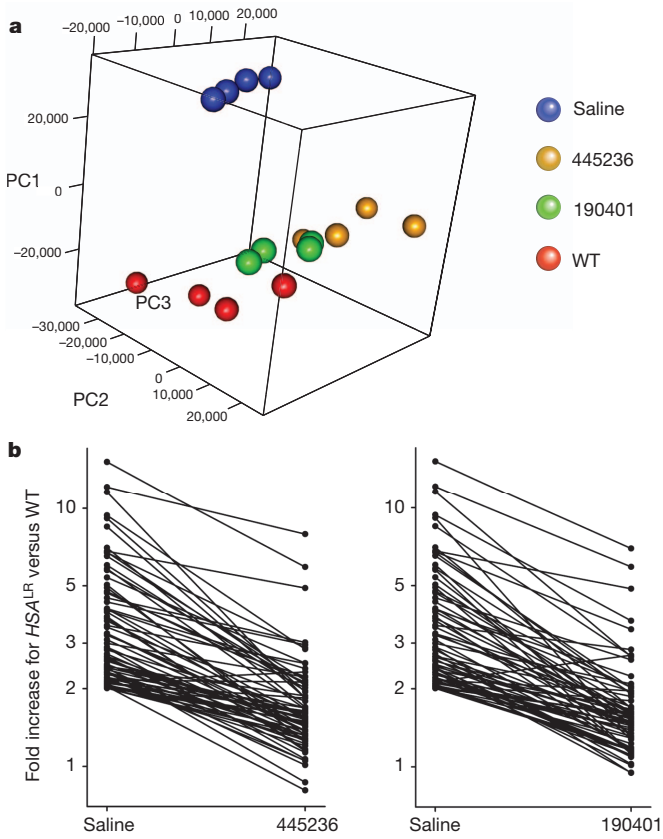

Figure 2 | Effects of ASOs on the transcriptome in quadriceps muscle. **a**, Principle component analysis of microarray data shows segregation of HSA^{LR} (saline) away from wild-type mice in widely separated clusters. ASOs caused HSA^{LR} transgenic mice to cluster nearer to wild-type mice (25 mg kg^{-1} biweekly for 4 weeks; $n = 4$ mice per group). **b**, Of the transcripts upregulated in HSA^{LR} versus wild-type mice (saline), >85% showed complete or partial return to normal expression after treatment with ASOs ($n = 4$ mice per group).

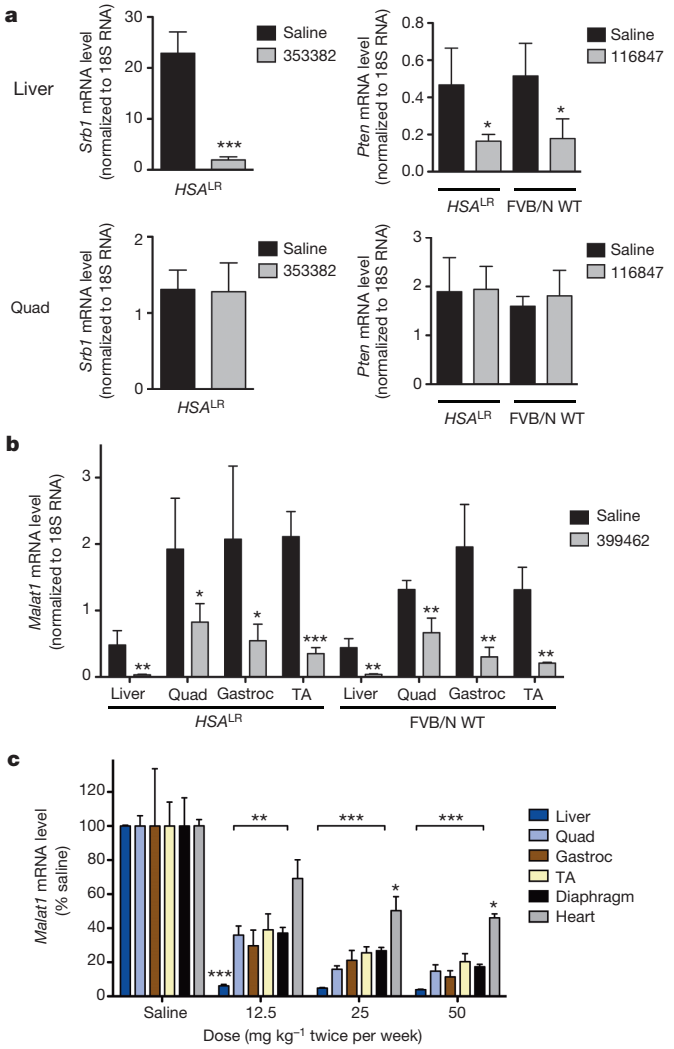

Figure 3 | Differential sensitivity of transcripts to ASO knockdown in skeletal muscle. **a**, In HSA^{LR} or FVB/N wild-type mice, ASOs targeting *Srb1* (353382) or *Pten* (116847) were effective for knockdown in liver but not in quadriceps muscle (qRT–PCR, $n = 4$ per group). Error bars are mean ± s.d. $^*P = 0.02$, $^{***}P < 0.0001$ (*t*-test). **b**, HSA^{LR} and FVB/N wild-type mice were treated with ASO 399462 targeting *Malat1*, a nuclear-retained lncRNA. Levels of *Malat1* transcript in the indicated tissues were determined by qRT–PCR ($n = 4$ ASO, 3 saline). Error bars are mean ± s.d. $^*P = 0.035$, $^{**}P < 0.007$, $^{***}P = 0.001$ for ASO versus saline (*t*-test). **c**, Dose response of *Malat1* knockdown in BALB/c wild-type mice. BALB/c wild-type mice were treated with saline or ASO 399462 targeting *Malat1* at 12.5, 25 and 50 mg kg^{-1} twice per week for 3.5 weeks (7 doses in total; $n = 4$ per group). Tissues were collected for RNA isolation 2 days after the final dose. *Malat1* transcript levels were determined by qRT–PCR. Error bars are mean ± s.e.m. $^*P < 0.01$, $^{**}P < 0.001$, $^{***}P < 0.0001$ (two-way ANOVA).

membrane, a physiological barrier to ASO uptake[24], and found that muscle penetration of the extracellular dye, Evans Blue, was similar in HSA^{LR} and wild-type mice (Supplementary Fig. 11a). Direct analysis of muscle tissue indicated that ASO accumulation was no greater in HSA^{LR} mice than in wild-type controls (Supplementary Fig. 11b, c). Likewise, the mRNA level for RNase H1 was similar in HSA^{LR} and wild-type muscle (Supplementary Fig. 12). We tested ASOs targeting other muscle-expressed transcripts. ASOs for *Pten* phosphatase or *Srb1* (also known as *Scarb1*) scavenger receptor showed efficient target knockdown in liver, but no appreciable knockdown in HSA^{LR} or wild-type muscle (Fig. 3a). Taken together with previous studies, our results indicate specific sensitivity of h*ACTA1*-CUG^{exp} transcripts rather than a general enhancement of ASO activity in HSA^{LR} muscle.

A notable metabolic feature of h*ACTA1*-CUG^{exp} and human *DMPK*-CUG^{exp} mRNA is that processing and polyadenylation are normal but the transcripts are retained in the nucleus[5,6]. Recent studies have shown that RNase H1, the enzyme responsible for antisense knockdown, is localized to the nucleus and mitochondria[14], suggesting that antisense cleavage of nuclear-encoded RNA occurs before nuclear export, and raising the possibility that nuclear-retained transcripts may exhibit enhanced sensitivity. To determine whether other nuclear-retained transcripts show a similar effect we examined metastasis associated lung adenocarcinoma transcript 1 (*Malat1*), an endogenous nuclear lncRNA[9]. We identified MOE gapmer ASOs that produced strong *Malat1* knockdown in cells, in an RNase H1-dependent manner (Supplementary Fig. 13). In wild-type and HSA^{LR} mice, subcutaneous administration of ASOs for 4 weeks caused a greater than 80% reduction in *Malat1* in muscle (Fig. 3b, c), supporting the idea that nuclear-retained transcripts have enhanced sensitivity.

To determine the duration of ASO action in muscle, we examined mice at 15 and 31 weeks after ASO was discontinued, and found that h*ACTA1*-CUG^{exp} knockdown and splicing correction remained strong (not shown). One year after ASO injection was discontinued, target reduction by ASO 190401 had waned, but remained approximately 50% or more for ASO 445236 (Fig. 4a). Even at this late time point the appropriate cleavage products were detected by amplification of complementary DNA 5′ ends (5′ RACE), indicating persistent ASO-RNase H1 activity (Fig. 4b). Consistent with the extent of target reduction, there was partial return of myotonia and splicing defects for

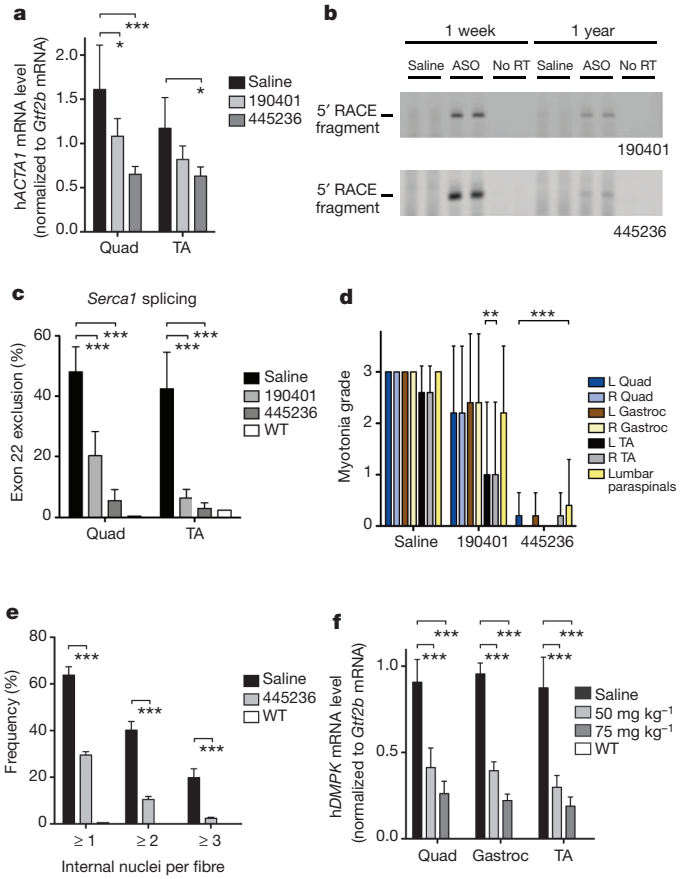

Figure 4 | Duration of ASO activity and *in vivo* targeting of human *DMPK*. **a–e**, Two-month-old HSA^{LR} mice received saline or ASO by subcutaneous injection of 25 mg kg^{-1} twice weekly for 4 weeks ($n = 5$ for each ASO, $n = 6$ for saline), with tissues isolated 1 year after the final dose. qRT–PCR analysis of HSA^{LR} transgene mRNA (mean ± s.d.) was normalized to the housekeeping gene *Gtf2b* mRNA (**a**). Results were similar when normalized to total RNA input. 5′ RACE was carried out on muscle RNA obtained 1 week or 1 year after discontinuation of ASO 190401 or 445236 treatment (**b**). PCR products (5′ RACE fragment) migrated at the expected position for ASO•RNase H cleavage products, and were confirmed by DNA sequencing. Quantification of *Serca1* splicing (**c**) and myotonia (**d**) showed a partial return of splicing defects and myotonia for ASO 190401 but not ASO 445236. Myotonia was graded blind by the examiner (**d**). After prolonged knockdown of toxic RNA, the number of internal nuclei per muscle fibre was determined by histologic analysis when mice were aged 14 months (**e**) ($n = 4$ for ASO 445236; $n = 3$ for saline; WT, untreated 3-month-old FVB/N wild-type control mice). **f**, DM328XL mice received subcutaneous injections of saline or ASO 445569 targeting the 3′ UTR of h*DMPK*. The ASO dose was 50 or 75 mg kg^{-1} twice weekly for 4 weeks ($n = 5$, low dose; $n = 4$, high dose; $n = 2$, saline). Tissues were isolated 2 days after the final dose. Dose-dependent reduction of h*DMPK*, normalized to housekeeping gene *Gtf2b* mRNA. Note that h*DMPK* mRNA was undetectable in wild-type mice. No RT, no reverse transcriptase. WT, untreated wild-type littermates of DM328XL transgenic mice ($n = 2$). Error bars are mean ± s.d. $^*P < 0.05$, $^{**}P < 0.001$, $^{***}P < 0.0001$ for ASO-treated versus saline-treated muscle (two-way ANOVA).

ASO 190401, whereas correction by ASO 445236 remained strong (Fig. 4c, d and Supplementary Fig. 14a–e). Furthermore, the persistent knockdown of CUG^{exp} RNA largely prevented the age-dependent myopathic changes in HSA^{LR} muscle, as evidenced by reduced frequency of central nuclei (Fig. 4e) and improved muscle-fibre diameter (mainly a prevention of fibre atrophy) (Supplementary Fig. 15). These findings indicate that ASO activity against h*ACTA1*-CUG^{exp} in muscle is remarkably durable and that long-term reduction of the toxic RNA can protect against structural changes in muscle fibres. Notably, the duration of *Malat1* knockdown in muscle was also prolonged (a greater than 50% reduction at 31 weeks after ASO discontinuation) and more persistent than in liver (Supplementary Fig. 16).

Therapeutic application of this strategy to human DM1 will require transfer of the targeting sequence to h*DMPK*. We developed MOE gapmer ASOs that were active against h*DMPK* in cells. We examined *in vivo* activity after 4 weeks of twice weekly subcutaneous injection in transgenic mice that express h*DMPK* with 800 CUG repeats. The ASO produced significant knockdown of h*DMPK*-CUG^{exp} transcripts in hindlimb muscle (Fig. 4f and Supplementary Figs 17 and 18), supporting the feasibility of silencing the pathogenic *DMPK* allele.

Despite physiological barriers to tissue uptake, our results indicate that systemic targeting of CUG^{exp} RNA is feasible because small amounts of ASOs that enter muscle fibres can hybridize their target and productively engage RNase H1. Although the mechanisms for enhanced sensitivity of CUG^{exp} RNA and *Malat1* are not fully defined, our data suggest that residence time in the nucleus is an important determinant of transcript sensitivity. Features of the nuclear environment that may enhance antisense activity include nuclear localization of RNase H1 (ref. 14) and auxiliary proteins that promote oligonucleotide hybridization[25], and—in the case of CUG^{exp} transcripts—spatial concentration of targets in a small volume[4]. A similar approach may be effective for other genetic disorders that have nuclear accumulation of repeat expansion RNA[26,27]. Previous studies have used CAG-repeat ASOs that bind CUG^{exp} RNA without activating RNase H, in an effort to block the protein interactions or modify the metabolism of the toxic RNA[18,28]. Although this approach was effective with local delivery, initial attempts at systemic delivery were less successful (T.M.W. and C.A.T., unpublished observations), which fits with the expectation that higher tissue concentrations of ASO are required to occupy CUG^{exp} binding sites than to induce RNase H cleavage. Furthermore, the RNase H mechanism is attractive because it exploits the nuclear retention phenomenon to gain a therapeutic advantage, while posing less risk of off-target effects by avoiding a repetitive sequence. Recently, local delivery of RNase H-active CAG-repeat ASOs induced partial CUG^{exp} knockdown, but was accompanied by muscle damage[29], again suggesting that direct targeting of the repeat tract may have pitfalls. Our results also suggest that ASOs are useful for *in vivo* functional characterization and therapeutic modulation of lncRNAs, a large and recently recognized class of regulatory RNAs[30].

METHODS SUMMARY

Experimental mice. All animal experiments were approved by the Institutional Animal Care and Use Committees at the University of Rochester, Genzyme Corporation and Isis Pharmaceuticals.

Subcutaneous injection of ASOs. MOE gapmer ASOs were dissolved in saline and administered by subcutaneous injection in the interscapular region twice per week at the indicated doses.

Quantitative real-time RT–PCR (polymerase chain reaction with reverse transcription) assay. Total RNA was purified from muscle using RNeasy Lipid Tissue Mini Kits (Qiagen). mRNA levels for *ACTA1*, *Srb1*, *Pten*, *Malat1* and RNase H1 were determined on the Applied Biosystems 7500 System using 18S rRNA as normalization control. General transcription factor 2b (*Gtf2b*) and total RNA (Ribogreen assay) served as normalization controls for human *DMPK* and mouse *Dmpk*.

Northern analysis. CUG^{exp} sequences were detected using a ^{32}P end-labelled $(CAG)_9$ DNA oligonucleotide probe.

Electromyography. Electromyography (EMG) was carried out blind under general anaesthesia, as described previously[18].

RT–PCR analysis of alternative splicing. RT–PCR was carried out using the SuperScript III One-Step RT–PCR System with Platinum Taq DNA Polymerase (Invitrogen) and the same gene-specific primers for cDNA synthesis and PCR amplification. PCR products were separated on agarose gels, stained with SybrGreen I Nucleic Acid Gel Stain (Invitrogen) and scanned with a fluorimager.

Transcriptome analysis. Quadriceps-muscle RNA from wild-type or HSA^{LR} transgenic mice treated with vehicle (saline), ASO 445236 or ASO 190401 was processed to cRNA and hybridized on microbeads using MouseRef-8 v2.0 Expression BeadChip Kits (Illumina). Image data were quantified using BeadStudio software (Illumina).

Full Methods and any associated references are available in the online version of the paper at www.nature.com/nature.

Received 7 September 2011; accepted 29 June 2012.

1. Harley, H. G. *et al.* Expansion of an unstable DNA region and phenotypic variation in myotonic dystrophy. *Nature* **355,** 545–546 (1992).
2. Buxton, J. *et al.* Detection of an unstable fragment of DNA specific to individuals with myotonic dystrophy. *Nature* **355,** 547–548 (1992).
3. Brook, J. D. *et al.* Molecular basis of myotonic dystrophy: expansion of a trinucleotide (CTG) repeat at the 3′ end of a transcript encoding a protein kinase family member. *Cell* **68,** 799–808 (1992).
4. Taneja, K. L., McCurrach, M., Schalling, M., Housman, D. & Singer, R. H. Foci of trinucleotide repeat transcripts in nuclei of myotonic dystrophy cells and tissues. *J. Cell Biol.* **128,** 995–1002 (1995).
5. Davis, B. M., McCurrach, M. E., Taneja, K. L., Singer, R. H. & Housman, D. E. Expansion of a CUG trinucleotide repeat in the 3′ untranslated region of myotonic dystrophy protein kinase transcripts results in nuclear retention of transcripts. *Proc. Natl Acad. Sci. USA* **94,** 7388–7393 (1997).
6. Mankodi, A. *et al.* Myotonic dystrophy in transgenic mice expressing an expanded CUG repeat. *Science* **289,** 1769–1773 (2000).
7. Bennett, C. F. & Swayze, E. E. RNA targeting therapeutics: molecular mechanisms of antisense oligonucleotides as a therapeutic platform. *Annu. Rev. Pharmacol. Toxicol.* **50,** 259–293 (2010).
8. Geary, R. S. *et al.* Pharmacokinetics of a tumor necrosis factor-alpha phosphorothioate 2′-*O*-(2-methoxyethyl) modified antisense oligonucleotide: comparison across species. *Drug Metab. Dispos.* **31,** 1419–1428 (2003).
9. Wilusz, J. E., Freier, S. M. & Spector, D. L. 3′ end processing of a long nuclear-retained noncoding RNA yields a tRNA-like cytoplasmic RNA. *Cell* **135,** 919–932 (2008).
10. Lorenz, P., Misteli, T., Baker, B. F., Bennett, C. F. & Spector, D. L. Nucleocytoplasmic shuttling: a novel *in vivo* property of antisense phosphorothioate oligodeoxynucleotides. *Nucleic Acids Res.* **28,** 582–592 (2000).
11. Vickers, T. A. *et al.* Efficient reduction of target RNAs by small interfering RNA and RNase H-dependent antisense agents. A comparative analysis. *J. Biol. Chem.* **278,** 7108–7118 (2003).
12. Prasanth, K. V. *et al.* Regulating gene expression through RNA nuclear retention. *Cell* **123,** 249–263 (2005).
13. Wu, H. *et al.* Determination of the role of the human RNase H1 in the pharmacology of DNA-like antisense drugs. *J. Biol. Chem.* **279,** 17181–17189 (2004).
14. Suzuki, Y. *et al.* An upstream open reading frame and the context of the two AUG codons affect the abundance of mitochondrial and nuclear RNase H1. *Mol. Cell. Biol.* **30,** 5123–5134 (2010).
15. Lin, X. *et al.* Failure of MBNL1-dependent post-natal splicing transitions in myotonic dystrophy. *Hum. Mol. Genet.* **15,** 2087–2097 (2006).
16. Osborne, R. J. *et al.* Transcriptional and post-transcriptional impact of toxic RNA in myotonic dystrophy. *Hum. Mol. Genet.* **18,** 1471–1481 (2009).
17. Kanadia, R. N. *et al.* A muscleblind knockout model for myotonic dystrophy. *Science* **302,** 1978–1980 (2003).
18. Wheeler, T. M. *et al.* Reversal of RNA dominance by displacement of protein sequestered on triplet repeat RNA. *Science* **325,** 336–339 (2009).
19. Hasselblatt, P., Hockenjos, B., Thoma, C., Blum, H. E. & Offensperger, W. B. Translation of stable hepadnaviral mRNA cleavage fragments induced by the action of phosphorothioate-modified antisense oligodeoxynucleotides. *Nucleic Acids Res.* **33,** 114–125 (2005).
20. Napierala, M. & Krzyzosiak, W. J. CUG repeats present in myotonin kinase RNA form metastable "slippery" hairpins. *J. Biol. Chem.* **272,** 31079–31085 (1997).
21. Miller, J. W. *et al.* Recruitment of human muscleblind proteins to (CUG)(n) expansions associated with myotonic dystrophy. *EMBO J.* **19,** 4439–4448 (2000).
22. Mankodi, A. *et al.* Expanded CUG repeats trigger aberrant splicing of ClC-1 chloride channel pre-mRNA and hyperexcitability of skeletal muscle in myotonic dystrophy. *Mol. Cell* **10,** 35–44 (2002).
23. Du, H. *et al.* Aberrant alternative splicing and extracellular matrix gene expression in mouse models of myotonic dystrophy. *Nature Struct. Mol. Biol.* **17,** 187–193 (2010).
24. Alter, J. *et al.* Systemic delivery of morpholino oligonucleotide restores dystrophin expression bodywide and improves dystrophic pathology. *Nature Med.* **12,** 175–177 (2006).
25. Pontius, B. W. & Berg, P. Rapid assembly and disassembly of complementary DNA strands through an equilibrium intermediate state mediated by A1 hnRNP protein. *J. Biol. Chem.* **267,** 13815–13818 (1992).
26. Li, L. B. & Bonini, N. M. Roles of trinucleotide-repeat RNA in neurological disease and degeneration. *Trends Neurosci.* **33,** 292–298 (2010).
27. DeJesus-Hernandez, M. *et al.* Expanded GGGGCC hexanucleotide repeat in noncoding region of C9ORF72 causes chromosome 9p-linked FTD and ALS. *Neuron* **72,** 245–256 (2011).
28. Mulders, S. A. *et al.* Triplet-repeat oligonucleotide-mediated reversal of RNA toxicity in myotonic dystrophy. *Proc. Natl Acad. Sci. USA* **106,** 13915–13920 (2009).
29. Lee, J. E., Bennett, C. F. & Cooper, T. A. RNase H-mediated degradation of toxic RNA in myotonic dystrophy type 1. *Proc. Natl Acad. Sci. USA* **109,** 4221–4226 (2012).
30. Wapinski, O. & Chang, H. Y. Long noncoding RNAs and human disease. *Trends Cell Biol.* **21,** 354–361 (2011).

Supplementary Information is linked to the online version of the paper at www.nature.com/nature.

Acknowledgements The work was carried out at the Wellstone Muscular Dystrophy Cooperative Research Center and Center for RNA Biology at the University of Rochester, with support from the US National Institutes of Health (NIH) (grants AR049077, U54NS48843, AR/NS48143, K08NS064293 and U01NS072323), the Saunders Family Neuromuscular Research Fund, Run America and a fellowship (to M.N.) from the Muscular Dystrophy Association and Uehara Memorial Foundation. The authors thank G. Gourdon for providing DM328XL mice, M. Sabripour for assistance with principal components analysis and L. Richardson and S. Leistman for technical assistance.

Author Contributions T.M.W., A.J.L, S.K.P., A.R.M., M.N., S.H.C., B.M.W., C.F.B. and C.A.T. participated in the planning, design and interpretation of experiments. T.M.W., A.J.L., S.K.P., A.R.M and M.N. carried out experiments. T.M.W. and C.A.T. wrote the manuscript.

Author Information Reprints and permissions information is available at www.nature.com/reprints. Readers are welcome to comment on the online version of this article at www.nature.com/nature. The authors declare competing financial interests: details accompany the full-text HTML version of the paper at www.nature.com/nature. Correspondence and requests for materials should be addressed to C.A.T. (charles_thornton@urmc.rochester.edu).

METHODS

Antisense oligonucleotides. ASOs were synthesized at Isis Pharmaceuticals, as described previously[31]. All ASOs were MOE gapmer 20mers with phosphorothioate as the intersubunit linkage, 2′-*O*-(2-methoxyethyl) (MOE) modifications of 5 nucleotides at the 5′ and 3′ end, and a central gap of 10 deoxynucleotides. The sequence of each ASO is listed in Supplementary Table 1. CAG25 and GAC25 morpholinos[18] were purchased (Gene Tools).

Identification of active ASOs. The criteria for identifying active h*ACTA1*-targeting ASOs were as follows: first, selection of targeting sequences that were not conserved in mice, to avoid knockdown of endogenous skeletal actin; second, >50% h*ACTA1* knockdown when electroporated in HepG2 cells (Supplementary Fig. 1); and third, absence of hepatotoxic or immunostimulatory effects in wild-type mice, when 50 mg kg^{-1} was injected subcutaneously twice weekly for 4 weeks (Supplementary Fig. 2a–c). Out of 11 candidate ASOs examined, 5 satisfied these criteria. For the ASO with the highest activity in HepG2 cells, we also verified activity against h*ACTA1*-CUG^{exp} transcripts *in vivo*, by direct injection and electroporation of tibialis anterior muscle in *HSA*^{LR} mice (Supplementary Fig. 3). Four of the five ASOs were subsequently used for subcutaneous administration in *HSA*^{LR} mice. ASOs targeting *Malat1* were identified by demonstration of >50% target knockdown when electroporated in mouse hepatocellular SV40 large T-antigen carcinoma (MHT) cells, and absence of hepatotoxic or immunostimulatory effects in wild-type mice (dosing as above).

Cell transfection and gene analysis. HepG2 cells were electroporated in a 96-well plate format at 165V with ASOs in complete media containing MEM, non-essential amino acid (NEAA), sodium pyruvate and 10% FBS at room temperature. Cells were incubated overnight and lysed in RLT buffer (Qiagen). Total RNA was prepared using Qiagen RNeasy kit. Quantitative real time RT–PCR (qRT–PCR) was performed using the Qiagen QuantiTect Probe RT–PCR kit. Twenty-microlitre qRT–PCR reactions were run in duplicate and normalized against total RNA, calculated using the Ribogreen assay (Invitrogen).

Experimental mice. Institutional Animal Care and Use Committees at the University of Rochester, Genzyme Corporation and Isis Pharmaceuticals approved all animal experiments. *HSA*^{LR} mice in the line 20b were derived and maintained on the FVB/N background strain[6]. The $(CTG)_{250}$ tract in this line is unstable, and has shortened to $(CTG)_{220}$. DM328XL mice carry a 45-kb human genomic fragment that includes the mutant *DMPK* gene with 800 CTG repeats[32,33]. The DM328XL mice were hemizygous and display no histologic changes, myotonia or splicing defects in skeletal muscle[34,35]. FVB/N, BALB/c, C57Bl/10 and Mdx mice were from Jackson Laboratories.

Muscle injection of ASOs. The tibialis anterior muscle was injected with 0.2, 0.4 or 0.8 nmol ASO in 20 µl saline, and the contralateral tibialis anterior with 20 µl saline alone, they were then electroporated, as described previously[36]. Treatment assignments were randomized and injections were carried out blind.

Subcutaneous injection of ASOs. All ASOs were dissolved in phosphate buffered saline (PBS). Doses of 2.5, 8.5, 12.5, 25 or 50 mg kg^{-1} were injected subcutaneously, twice per week in the interscapular region for 3.5 to 4 weeks (7 or 8 doses in total). Injection volumes ranged from 140 to 200 µl.

Real-time PCR Assay. Total RNA was purified from tibialis anterior, gastrocnemius or quadriceps muscle using the RNeasy Lipid Tissue Mini Kit (Qiagen) according to the manufacturer's instructions. qRT–PCR was used to determine mRNA levels for *ACTA1*, *Srb1*, *Pten*, *Malat1* and *RNase H1*, with 18S rRNA as normalization control, on an Applied Biosystems 7500 Real-Time PCR System. *Gtf2b* and total RNA (Ribogreen assay) served as normalization controls for human *DMPK* and mouse *Dmpk*.

Real-time PCR assay primer probe set sequences. *ACTA1* primer probe set 1 (PPset 1): forward, 5′-GTAGCTACCCGCCCAGAAACT-3′; reverse, 5′-CCA GGCCGGAGCCATT-3′; probe, 5′-ACCACCGCCCTCGTGTGCG-3′. *ACTA1* PPset 2: forward, 5′-GACGAGGCTCAGAGCAAGAGA-3′; reverse, 5′-TGATG ATGCCGTGCTCGATA-3′; probe, 5′-CCTGACCCTGAAGTAC-3′. *Srb1*: forward, 5′-TGACAACGACACCGTGTCCT-3′; reverse, 5′-ATGCGACTTGTC AGGCTGG-3′; probe, 5′-CGTGGAGAACCGCAGCCTCCATT-3′. *Pten*: forward, 5′-ATGACAATCATGTTGCAGCAATTC-3′; reverse: 5′-CGATGCA ATAAATATGCACAAATCA-3′; probe, 5′-CTGTAAAGCTGGAAAGGGACG GACTGGT-3′. *Malat1*: forward, 5′-TGGGTTAGAGAAGGCGTGTACTG-3′; reverse, 5′-TCAGCGGCAACTGGGAAA-3′; probe, 5′-CGTTGGCACGACAC CTTCAGGGACT-3′. RNase H1: forward, 5′-ACTCAGGATTTGTGGGCAA TG-3′; reverse, 5′-CCTCAGACTGCTTCGCTCCTT-3′; probe, 5′-AGAGGC CGACAGACTGGCACGG-3′. Human *DMPK*: forward, 5′-AGCCTGAGCC GGGAGATG-3′; reverse, 5′-GCGTAGTTGACTGGCGAAGTT-3′; probe, 5′-AGGCCATCCGCACGGACAACCX-3′. Mouse *Dmpk*: forward, 5′-GACAT ATGCCAAGATTGTGCACTAC-3′; reverse: 5′-CACGAATGAGGTCCTGAG CTT-3′; probe, 5′-AACACTTGTCGCTGCCGCTGGCX-3′. *Ap2M1*, sequences previously reported[37]. 18S rRNA, proprietary sequences (Applied Biosystems, catalogue number 4310893-E). *Gtf2b*, proprietary sequences (Applied Biosystems, catalogue number 4331182)

Northern analysis. Total RNA (6 µg) was separated on agarose gels containing MOPS and formaldehyde, transferred to nylon membranes and hybridized with $(CAG)_9$ or mouse actin ^{32}P-labelled oligonucleotide probes, as described previously[18].

Electromyography. EMG was carried out blind under anaesthesia, as described previously[18]. Myotonic discharges were graded on a four-point scale: 0, no myotonia; 1, occasional myotonic discharge in less than 50% of needle insertions; 2, myotonic discharge in greater than 50% of needle insertions; 3, myotonic discharge with nearly every insertion.

RT–PCR analysis of alternative splicing. RT–PCR was carried out using the SuperScript III One-Step RT–PCR with Platinum Taq DNA Polymerase (Invitrogen) using gene-specific primers for cDNA synthesis and PCR amplification. The primers for *Clcn1*, *Serca1*, *Titin* and *Zasp* were described previously[15,36]. PCR products were separated on agarose gels, stained with SybrGreen I Nucleic Acid Gel Stain (Invitrogen) and imaged using a laser scanner (Fujifilm LAS-3000 Intelligent Dark Box or GE Healthcare Typhoon 9400). Band intensities were quantified using ImageQuant software (GE Healthcare.)

Transcriptome analysis by microarray. RNA was isolated from quadriceps muscle of wild-type mice or *HSA*^{LR} transgenic mice treated with vehicle (saline), ASO 445236 or ASO 190401 ($n = 4$ per group, 25 mg kg^{-1} ASO twice weekly for 4 weeks). RNA integrity was verified (RIN values >7.5 on Agilent Bioanalyzer). RNA was processed to cRNA and hybridized on microbeads using MouseRef-8 v2.0 Expression BeadChip Kits (Illumina) according to the manufacturer's recommendations. Image data were quantified using BeadStudio software (Illumina). Signal intensities were quantile normalized. We used row-specific offsets to avoid any values of less than two, before the normalization. Data from all probe sets with six or more nucleotides of CUG, UGC or GCU repeats were suppressed to eliminate the possibility that expanded repeats in the hybridization mixture (CAG repeats in cRNA, originating from CUG^{exp} RNA) could cross-hybridize with repeat sequences on probes. To eliminate genes whose expression was not readily quantified on the arrays, we suppressed probes that did not show a detection probability of $P < 0.1$ for all samples in the group that showed the higher mean expression level. Comparisons between groups were summarized and rank ordered by fold-changes of mean expression level and *t*-tests. The software package *R* (ref. 38) was used to perform principal components analysis (PCA)[39,40] on wild-type, ASO-treated, and saline-treated microarray samples. The principal components allowed the capture of the majority of the expression variation in each sample within three dimensions. We plotted the first three principal components of each sample. Array data have been submitted to the Gene Expression Omnibus, accession number GSE38962 (http://www.ncbi.nlm.nih.gov/geo/query/acc.cgi?acc=GSE38962).

Fluorescence *in situ* hybridization. Localization of CUG^{exp} RNA by fluorescence *in situ* hybridization (FISH) was carried out using a CAG repeat oligoribonucleotide probe labelled with Texas Red at the 5′ end, on muscle cryosections from ASO- or saline-treated mice, as described previously[15]. Images are maximum projections of deconvolved Z-plane stacks (9 images, 0.1- or 0.2-µM steps) captured under identical exposure and illumination conditions using a fluorescence microscope (Carl Zeiss Axioplan 2 or Nikon Eclipse E600), a charge-coupled device (CCD) digital camera (Hamamatsu ORCA R2 or Photometrics Cool Snap HQ) and Metamorph software (Molecular Devices). The Optigrid structured illumination imaging system (Qioptiq) was also used to capture images of DM328XL muscle. Maximum grey-level intensity was quantified using Metamorph. Objectives: ×100 Plan-APOCHROMAT 1.4 NA oil (Zeiss) or ×60 Plan Apo 1.4 NA oil (Nikon).

Muscle-fibre morphometry. To outline muscle fibres and label nuclei, 10-µM transverse cryosections of muscles from ASO- or saline-treated mice were fixed with 4% paraformaldehyde, pH 7.3, washed in PBS and incubated in 20 µg ml^{-1} FITC-wheat germ agglutinin (WGA; Sigma) and 4,6 diamino-2 phenylindole dihydrochloride (DAPI; 1:20,000) in PBS for 1 h at room temperature. Sections then were washed in PBS, mounted and sealed. Images were captured using an Axioplan 2 fluorescence microscope (Zeiss), an ORCA R2 CCD digital camera (Hamamatsu Photonics), Metamorph software and a ×20 Plan-NEOFLUAR 0.5 NA objective (Zeiss). Using the calipers application in Metamorph, the muscle-fibre diameter, defined as the minimum 'Feret's diameter' (the mimimum distance of parallel tangents at opposing borders of the muscle fibre[41]), was determined. Haematoxylin and eosin (H&E)-stained images were captured using an Infinity*2-1* 1.4 megapixel colour CCD digital camera (Lumenera), Infinity Analyze 5.0 software (Lumenera) and a ×10 Plan-NEOFLUAR 0.3 NA objective (Zeiss).

5′ rapid amplification of cDNA ends analysis. 5′ rapid amplification of cDNA ends (RACE) was carried out using the FirstChoice RLM-RACE Kit (Invitrogen). In brief, 1 µg of total mRNA was ligated with 5′ RACE adaptor (5′-GCUGAUGGCGAUGAAUGAACACUGCGUUUGCUGGCUUUGAUGA

AA-3′), then reverse transcribed with a primer specific for the cleavage fragment (5′-TGAGAAGTCGCGTGCTGGAG-3′ for 190401, or 5′-TTTTTTTTACGCAGC-3′ for 445236). The synthesized cDNA was treated with RNase H, then amplified with 5′ RACE Outer Primer and 5′-TTGCGGTGGACGATGGAAGG-3′ (for 190401 fragment), or 5′-TGTGTAAAACGACGGCCAGTACGCAGCTTAACAGAATGAC-3′ (for 445236 fragment). The PCR products were analysed on agarose gels stained with SYBR Green I (Invitrogen) and scanned with a laser fluorimager (Typhoon, GE Healthcare).

RNase H1 short interfering RNA experiments. MHT cells were cultured in DMEM supplemented with 10% fetal calf serum, streptomycin (0.1 mg ml^{-1}), and penicillin (100 U ml^{-1}). Short interfering RNA (siRNA) treatments were carried out using Opti-MEM containing 5 mg ml^{-1} Lipofectamine 2000, as previously described[37]. In brief, MHT cells were plated with 7,500 cells per well and were incubated for either 24 or 48 h with 75 nM of siRNA targeting RNaseH1 (5′-GCTTGGTGAGACGTGCTTATT-3′ and 5′-TAAGCACGTCTCACCAAGCTG-3′) or *Ap2M1* (sequences reported previously[37]) in OPTI-MEM and Lipofectamine 2000. Twenty-four hours post transfection, cells were treated with increasing doses of the *Malat1*-targeting ASO 399479 in DMEM–10% FBS. Twenty-four hours after the addition of oligonucleotides, cells were lysed and RNA was isolated using RNAeasy and qRT–PCR was performed to determine the level of *Malat1* mRNA.

Tissue drug-level determination. Approximately 30 to100 mg liver and muscle tissue were homogenized as described[42]. Capillary gel electrophoresis (CGE) methods were used to measure unlabelled drug concentrations in mouse tissues. The methods for the h*ACTA1* ASOs were slight modifications of previously published methods[42,43], and consisted of a phenol–chloroform (liquid–liquid) extraction followed by a solid-phase extraction. An internal standard (ASO 355868, a 27mer 2′-*O*-methoxyethyl-modified phosphorothioate oligonucleotide) was added before extraction. Tissue sample analyses were conducted using a Beckman MDQ capillary electrophoresis instrument (Beckman Coulter). Tissue-sample concentrations were calculated using calibration curves, with a lower limit of quantification (LLoQ) of approximately 1.14 μg g^{-1}.

Biochemical analysis and serum chemistry. Serum separated in serum separator tubes (BD catalogue number 365956) was used to determine aspartate transaminase (AST), alanine transaminase (ALT), blood urea nitrogen (BUN) and creatinine values using Olympus reagents and an Olympus AU400e analyser (Melville).

Evans blue dye uptake assay. Evans blue dye (EBD) was dissolved in PBS at a concentration of 10 mg ml^{-1} and filter-sterilized. *HSA*^{LR}, FVB/N, Mdx or C57Bl/10 mice were administered an intraperitoneal injection of 10 μl EBD solution per gram of bodyweight. After a period of 24 h, muscle tissues were collected (quadriceps, gastrocnemius, tibialis anterior, diaphragm and heart). The mass of each muscle was recorded before lysing each sample individually in a microfuge tube containing *N*,*N*-dimethylformamide and a 5-mm steel bead, which was subjected to 30 Hz shaking in a Qiagen TissueLyser II. Lysed muscle samples were heated at 55 °C and centrifuged, and the absorbance of the supernatant was determined by spectrophotometric measurement at 636 nm. A standard curve of EBD in *N*,*N*-dimethylformamide enabled the EBD content in individual muscle samples to be determined.

Statistical analysis. Group data are presented as mean ± s.d., except where mean ± s.e.m. is indicated. Between-group comparison was carried out using a two-tailed Student's *t*-test or an analysis of variance (ANOVA), as indicated. A P value of <0.05 was considered significant.

31. Cheruvallath, Z. S., Kumar, R. K., Rentel, C., Cole, D. L. & Ravikumar, V. T. Solid phase synthesis of phosphorothioate oligonucleotides utilizing diethyldithiocarbonate disulfide (DDD) as an efficient sulfur transfer reagent. *Nucleosides Nucleotides Nucleic Acids* **22,** 461–468 (2003).
32. Seznec, H. *et al.* Transgenic mice carrying large human genomic sequences with expanded CTG repeat mimic closely the DM CTG repeat intergenerational and somatic instability. *Hum. Mol. Genet.* **9,** 1185–1194 (2000).
33. Nakamori, M., Gourdon, G. & Thornton, C. A. Stabilization of expanded (CTG)*(CAG) repeats by antisense oligonucleotides. *Mol. Ther.* **19,** 2222–2227 (2011).
34. Seznec, H. *et al.* Mice transgenic for the human myotonic dystrophy region with expanded CTG repeats display muscular and brain abnormalities. *Hum. Mol. Genet.* **10,** 2717–2726 (2001).
35. Gomes-Pereira, M. *et al.* CTG trinucleotide repeat ''big jumps'': large expansions, small mice. *PLoS Genet.* **3,** e52 (2007).
36. Wheeler, T. M., Lueck, J. D., Swanson, M. S., Dirksen, R. T. & Thornton, C. A. Correction of ClC-1 splicing eliminates chloride channelopathy and myotonia in mouse models of myotonic dystrophy. *J. Clin. Invest.* **117,** 3952–3957 (2007).
37. Koller, E. *et al.* Mechanisms of single-stranded phosphorothioate modified antisense oligonucleotide accumulation in hepatocytes. *Nucleic Acids Res.* **39,** 4795–4807 (2011).
38. Ihaka, R. & Gentleman, R. R. A language for data analysis and graphics. *J. Comput. Graph. Stat.* **5,** 299–314 (1996).
39. Raychaudhuri, S., Stuart, J. M. & Altman, R. B. Principal components analysis to summarize microarray experiments: application to sporulation time series. *Pac. Symp. Biocomput.* **2000,** 455–466 (2000).
40. Ringnér, M. What is principal component analysis? *Nature Biotechnol.* **26,** 303–304 (2008).
41. Briguet, A., Courdier-Fruh, I., Foster, M., Meier, T. & Magyar, J. P. Histological parameters for the quantitative assessment of muscular dystrophy in the *mdx*-mouse. *Neuromuscul. Disord.* **14,** 675–682 (2004).
42. Leeds, J. M., Graham, M. J., Truong, L. & Cummins, L. L. Quantitation of phosphorothioate oligonucleotides in human plasma. *Anal. Biochem.* **235,** 36–43 (1996).
43. Geary, R. S., Matson, J. & Levin, A. A. A nonradioisotope biomedical assay for intact oligonucleotide and its chain-shortened metabolites used for determination of exposure and elimination half-life of antisense drugs in tissue. *Anal. Biochem.* **274,** 241–248 (1999).